Supplementary information for

Multi-scale phase separation in poly(D,L-lactide-*co*-glycolide) and palmitic acid blends using neutron and X-ray scattering

Caitlyn M. Wolf[1,*], Robert M. Dalgliesh[2], Liliana de Campo[3], Gregory N. Smith[2], Katie M. Weigandt[1,*]

[1]NIST Center for Neutron Research, National Institute of Standards and Technology, Gaithersburg, MD 20899, United States

[2]ISIS Neutron Muon Source, Science and Technology Facilities Council, Rutherford Appleton Laboratory, Didcot OX11 0QX, United Kingdom

[3]Australian Centre for Neutron Scattering (ACNS), ANSTO, Lucas Heights, NSW 2234, Australia

**corresponding authors*

**Email: caitlyn.wolf@nist.gov*

**Email: kathleen.weigandt@nist.gov*

1. SANS data fits

The knee feature in the SANS spectra shown in Figure 1 of the main manuscript was fit with a sphere or ellipsoid form factor depending on whether one or two slope changes were observed within the feature, respectively. A power law model was combined with the form factor to account for the scattering intensity at the low q-values from larger structures captures in the USANS spectra. Therefore, each SANS spectra was fit with a combined power law and sphere model or a combined power law and ellipsoid model after subtracting the incoherent background.

The incoherent background was determined by fitting a power law model with a flat background at q-values above 0.035 Å^{-1}. The data in the incoherent regime was not perfectly flat due to the wide range of wavelengths used to measure the sample from 3 Å to 13 Å for samples at 10 % palmitic acid and higher or from wavelengths of 3 Å to 18 Å for samples with less that 10 % palmitic acid. Therefore, a slight over or under subtraction can be seen in the Porod region of the sphere and ellipsoid fits. We note this limitation but ensure that the primary slope changes indicative of length scale, either the sphere radius or the ellipsoid polar and equatorial radii, can still be captured by the model.

The combined model fits overlaid on the SANS spectra are shown in Figures S1, S2, S3 and S4 and all model parameters are provided in Tables S1, S2, S3, and S4. All fits were performed using SasView and model parameters with a prefix of "A_" refer to the power law portion of the model and parameters with a prefix of "B_" refer to either the sphere or ellipsoid portion of the model. We refer to the SasView documentation for a thorough description of all parameters.[1]

The models were combined using the following two equations:

$$I(q) = scale * \left(I_{power\ law}(q) + I_{sphere}(q)\right) + background \quad \text{(S1)}$$

$$I(q) = scale * \left(I_{power\ law}(q) + I_{ellipsoid}(q)\right) + background \quad \text{(S2)}$$

where $scale$ is a generic scaling parameter fixed at 1, $background$ is the incoherent background fixed at 0, and $I_{model\ name}$ is the scattering intensity from the individual power law, sphere, or ellipsoid model.

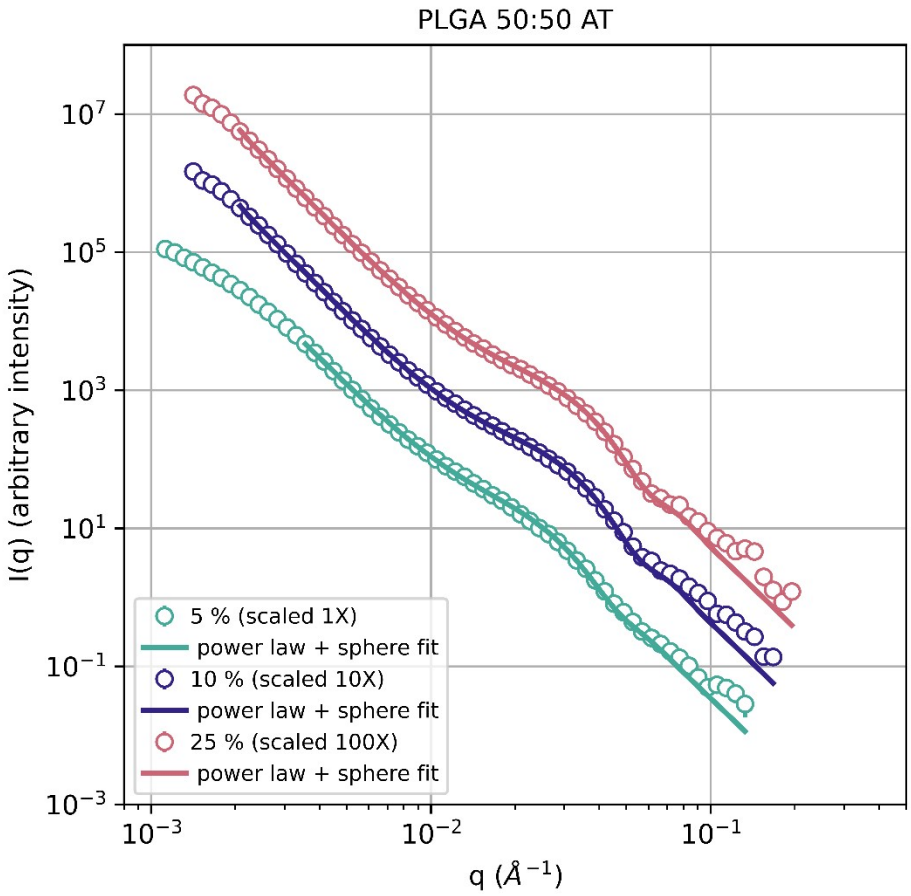

Figure S1. Fits of a combined power law and sphere model to SANS data for a blend of acid-terminated PLGA 50:50 and palmitic-d_{31} acid at mass fractions from 5 % to 25 % shown in Figure 1a of the main manuscript. The data and model fit at 10 % and 25 % were scaled for improved visibility.

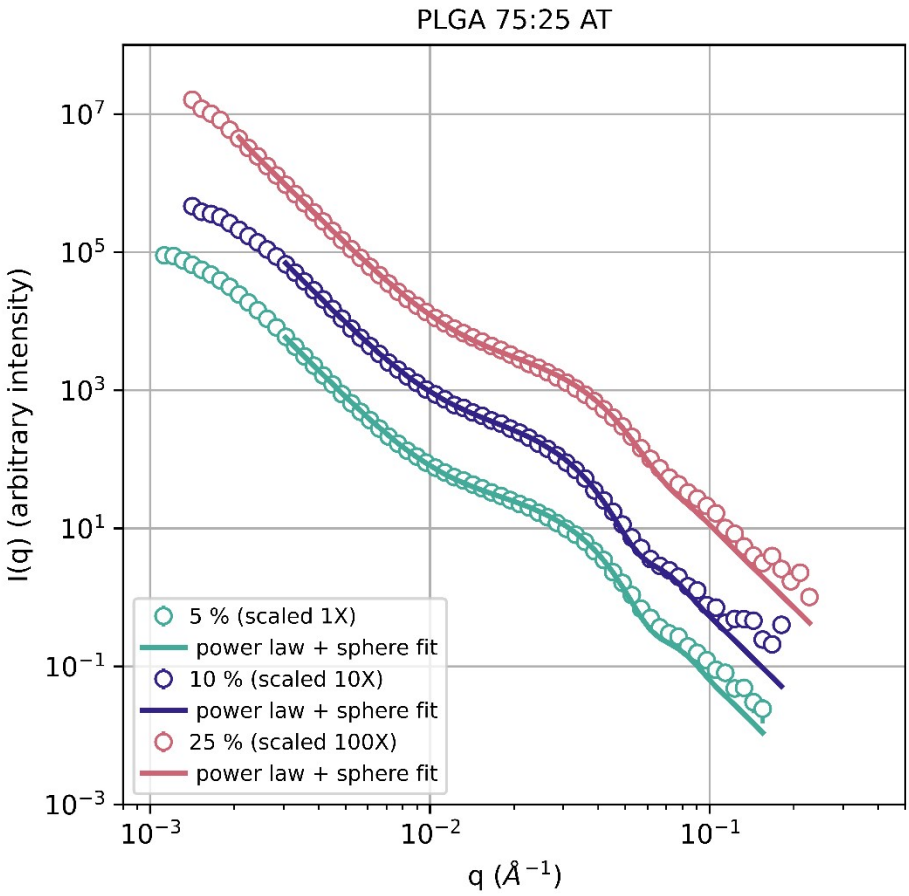

Figure S2. Fits of a combined power law and sphere model to SANS data for a blend of acid-terminated PLGA 75:25 and palmitic-d_{31} acid at mass fractions from 5 % to 25 % shown in Figure 1b of the main manuscript. The data and model fit at 10 % and 25 % were scaled for improved visibility.

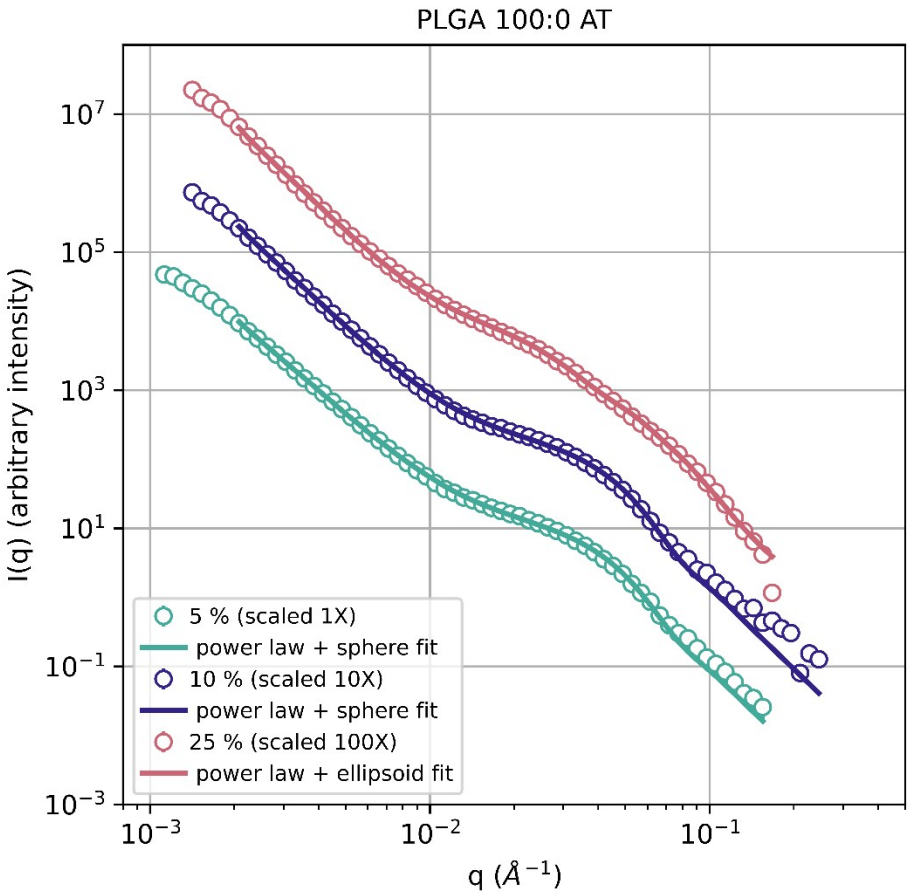

Figure S3. Fits of a combined power law and sphere model or combined power law and ellipsoid model to SANS data for a blend of acid-terminated PLGA 100:0 and palmitic-d_{31} acid at mass fractions from 5 % to 25 % shown in Figure 1c of the main manuscript. The data and model fit at 10 % and 25 % were scaled for improved visibility.

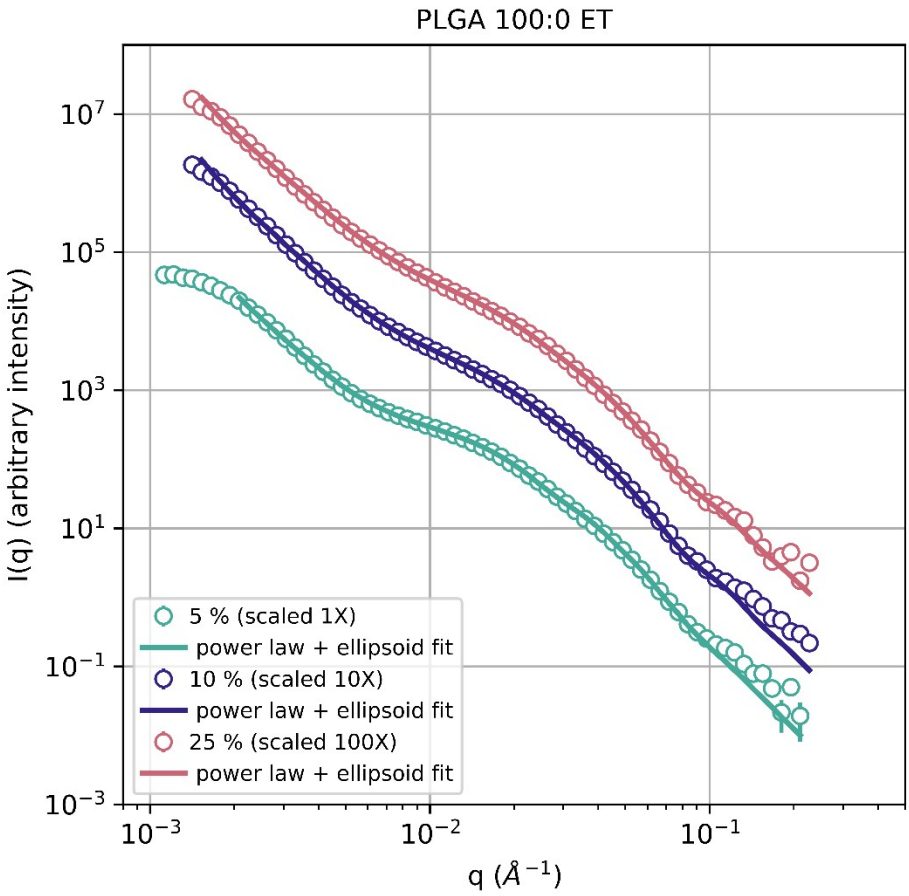

Figure S4. Fits of a combined power law and ellipsoid model to SANS data for a blend of ester-terminated PLGA 100:0 and palmitic-d_{31} acid at mass fractions from 5 % to 25 % shown in Figure 1d of the main manuscript. The data and model fit at 10 % and 25 % were scaled for improved visibility.

Table S1. Power law and sphere parameters from model fits to SANS data shown in Figure S1. Parameters allowed to vary during the fit include a standard error from the fitting algorithm.

Parameter (units)	Mass Fraction of Palmitic Acid		
	5 %	**10 %**	**25 %**
Model	power law + sphere	power law + sphere	power law + sphere
scale	1	1	1
background (cm^{-1})	0	0	0
A_scale	3.4e-06 ± 1e-07	2.79e-06 ± 4e-08	3.78e-06 ± 5e-08
A_power	3.679 ± 0.007	3.722 ± 0.002	3.708 ± 0.002
B_scale	0.00397 ± 4e-05	0.00542 ± 2e-05	0.00612 ± 3e-05
B_sld (10^{-6} Å^{-2})	1.86	1.86	1.86
B_sld_solvent (10^{-6} Å^{-2})	6.41	6.41	6.41
B_radius (Å)	81.0 ± 0.3	72.7 ± 0.2	67.9 ± 0.2
B_radius_pd	0.25	0.2	0.2

Table S2. Power law and sphere parameters from model fits to SANS data shown in Figure S2. Parameters allowed to vary during the fit include a standard error from the fitting algorithm.

Parameter (units)	Mass Fraction of Palmitic Acid		
	5 %	**10 %**	**25 %**
Model	power law + sphere	power law + sphere	power law + sphere
scale	1	1	1
background (cm^{-1})	0	0	0
A_scale	1.38e-06 ± 5e-08	2.01e-06 ± 7e-08	4.09e-06 ± 6e-08
A_power	3.766 ± 0.007	3.725 ± 0.007	3.66 ± 0.002
B_scale	0.00889 ± 4e-05	0.00768 ± 4e-05	0.01267 ± 4e-05
B_sld (10^{-6} Å^{-2})	1.69	1.69	1.69
B_sld_solvent (10^{-6} Å^{-2})	6.41	6.41	6.41
B_radius (Å)	65.7 ± 0.2	72.7 ± 0.2	52.08 ± 0.09
B_radius_pd	0.2	0.2	0.3

Table S3. Power law and sphere parameters or power law and ellipsoid parameters from model fits to SANS data shown in Figure S3. Parameters allowed to vary during the fit include a standard error from the fitting algorithm.

Parameter (units)	**Mass Fraction of Palmitic Acid**		
	5 %	**10 %**	**25 %**
Model	power law + sphere	power law + sphere	power law + ellipsoid
scale	1	1	1
background (cm^{-1})	0	0	0
A_scale	9.5e-06 ± 3e-07	8.1e-06 ± 1e-07	9.2e-06 ± 2e-07
A_power	3.307 ± 0.005	3.449 ± 0.003	3.584 ± 0.003
B_scale	0.00758 ± 4e-05	0.01256 ± 4e-05	0.027 ± 0.0001
B_sld (10^{-6} Å^{-2})	1.52	1.52	1.52
B_sld_solvent (10^{-6} Å^{-2})	6.41	6.41	6.41
B_radius (Å)	45.3 ± 0.1	44.6 ± 0.08	
B_radius_pd	0.3	0.3	
B_radius_polar (Å)			26.1 ± 0.1
B_radius_polar_pd			0.2
B_radius_equatorial (Å)			117.7 ± 0.5
B_radius_equatorial_pd			0

Table S4. Power law and ellipsoid parameters from model fits to SANS data shown in Figure S4. Parameters allowed to vary during the fit include a standard error from the fitting algorithm.

Parameter (units)	**Mass Fraction of Palmitic Acid**		
	5 %	**10 %**	**25 %**
Model	power law + ellipsoid	power law + ellipsoid	power law + ellipsoid
scale	1	1	1
background (cm^{-1})	0	0	0
A_scale	3.4e-06 ± 2e-07	1.59e-05 ± 4e-07	4.2e-05 ± 1e-06
A_power	3.592 ± 0.008	3.48 ± 0.004	3.305 ± 0.004
B_scale	0.0286 ± 7e-05	0.0277 ± 8e-05	0.0259 ± 0.0001
B_sld (10^{-6} Å^{-2})	1.52	1.52	1.52
B_sld_solvent (10^{-6} Å^{-2})	6.41	6.41	6.41
B_radius_polar (Å)	41.4 ± 0.1	45.5 ± 0.1	45.5 ± 0.2
B_radius_polar_pd	0.2	0.1	0.1
B_radius_equatorial (Å)	168.6 ± 0.5	159.6 ± 0.6	150.0 ± 0.7
B_radius_equatorial_pd	0	0.2	0.2

2. SESANS model parameters

An ellipsoid form factor[2] or spinodal model [3–5] as implemented in SasView[1] were fit to the SESANS data. The parameters for all model fits to the SESANS data are provided below in Table S5, Table S6, Table S7, and Table S8. Any parameters allowed to vary during the fit include a standard error from the fitting algorithm. The remaining parameters were held constant at the values shown. In samples at palmitic acid loadings of 10 % or 25 %, contrast was modulated in the SESANS samples by blending PA-d_{31} and fully hydrogenated palmitic acid at PA-d_{31} mass fractions of 79 % and 65 %, respectively. Therefore, the scattering length density term for palmitic acid in the ellipsoid fits has been adjusted accordingly and are shown in the parameter tables of this section. The data and model fits shown in the main manuscript were rescaled to full contrast (assuming PA-d_{31} is the only dispersed molecule) to enable direct comparison on an absolute scale between spectra for samples with different loadings of palmitic acid.

Table S5. Ellipsoid form factor parameters from model fits to SESANS data shown in Figure 5a of the main manuscript for blends comprised of an acid-terminated PLGA 50:50 matrix and dispersed palmitic acid. Parameters allowed to vary during the fit include a standard error from the fitting algorithm.

Parameter (units)	**Mass Fraction of Palmitic Acid**		
	5 %	**10 %**	**25 %**
scale	0.006 ± 0.001	0.012 ± 0.001	0.025 ± 0.002
background (cm^{-1})	0	0	0
sld (10^{-6} Å^{-2})	6.41	5.06	4.15
sld_solvent (10^{-6} Å^{-2})	1.86	1.86	1.86
radius_polar (Å)	200000	200000	200000
radius_polar_pd	0	0	0
radius_equatorial (Å)	920 ± 180	1550 ± 180	2170 ± 180
radius_equatorial_pd_n	0.2	0.2	0.2
radius_equatorial_pd_nsigma	35	35	35
radius_equatorial_pd_type	3	3	3

Table S6. Ellipsoid form factor parameters from model fits to SESANS data shown in Figure 5b of the main manuscript for blends comprised of an acid-terminated PLGA 75:25 matrix and dispersed palmitic acid. Parameters allowed to vary during the fit include a standard error from the fitting algorithm.

Parameter (units)	Mass Fraction of Palmitic Acid	
	10 %	**25 %**
scale	0.015 ± 0.002	0.021 ± 0.003
background (cm^{-1})	0	0
sld (10^{-6} Å^{-2})	5.06	4.15
sld_solvent (10^{-6} Å^{-2})	1.70	1.70
radius_polar (Å)	200000	200000
radius_polar_pd	0	0
radius_equatorial (Å)	890 ± 150	1290 ± 190
radius_equatorial_pd_n	0.2	0.2
radius_equatorial_pd_nsigma	35	35
radius_equatorial_pd_type	3	3

Table S7. Spinodal model parameters from fits to SESANS data shown in Figure 5c of the main manuscript for blends comprised of an acid-terminated PLGA 100:0 matrix and dispersed palmitic acid. Parameters allowed to vary during the fit include a standard error from the fitting algorithm.

Parameter (units)	Mass Fraction of Palmitic Acid
	25 %
scale	5329832 ± 794283
background (cm^{-1})	0
gamma	2.9 ± 0.1
q_0 (Å^{-1})	0.00020 ± 0.00002

Table S8. Spinodal model parameters from fits to SESANS data shown in Figure 5d of the main manuscript for blends comprised of an ester-terminated PLGA 100:0 matrix and dispersed palmitic acid. Parameters allowed to vary during the fit include a standard error from the fitting algorithm.

Parameter (units)	**Mass Fraction of Palmitic Acid**	
	10 %	**25 %**
scale	3288990 ± 497123	4814295 ± 638849
background (cm^{-1})	0	0
gamma	2.8 ± 0.1	3.0 ± 0.1
q_0 ($Å^{-1}$)	0.00026 ± 0.00003	0.00023 ± 0.00002

3. WAXS analysis

The WAXS spectra were analyzed by fitting a series of multiple Gaussians to the sharp crystalline and broad amorphous peaks from the palmitic acid, polymer matrix, and Kapton holder. A multi-Gaussian fit to the Kapton holder is shown in Figure S5(a). Each individual Gaussian is shown as a different color and the combined multi-Gaussian model is shown in a solid black line overlaying the measured data shown in markers. In subsequent fits of samples, the Kapton combined fit is scaled appropriately, as shown in the purple line of Figure S5(b, c), without modifying the relative intensities of the individual Gaussian components. Additional Gaussian peaks are then added to fit the amorphous polymer matrix. These are shown in Figure S5(b, c). Similarly, these multi-Gaussian fits to the polymer matrix are scalable in fits to the samples containing palmitic acid. Additional Gaussians are added to the model to fit the crystalline peaks arising from the added phase, as shown in the main manuscript.

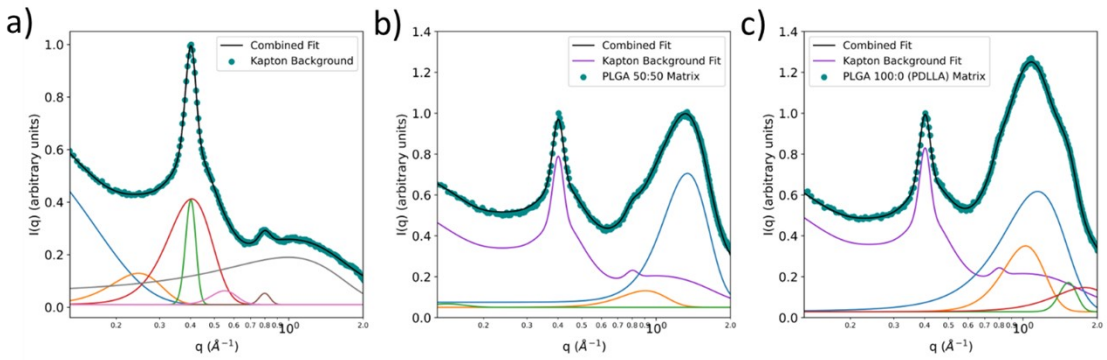

Figure S5. Wide-angle X-ray scattering measurements of (a) Kapton film sample holder and (b-c) matrix polymer samples of PLGA at varying lactide:glycolide ratios of 50:50 or 100:0 wrapped in Kapton, respectively, fit with multiple Gaussian functions. In panel (a) the colored lines are summed resulting in the combined fit shown overlaid on the experimental data (cyan markers). This Kapton background fit is shown in (b) and (c) as the purple line. In (b) and (c), the remaining colored lines are summed with the background Kapton resulting in the combined fit shown overlaid on the experimental data (cyan markers). This combined fit is representative of scattering from both the Kapton film and the matrix polymer. All experimental data was normalized to the primary Kapton peak at approximately 0.42 $Å^{-1}$.

4. References

1 M. Doucet, J. H. Cho, G. Alina, Z. Attala, J. Bakker, P. Beaucage, W. Bouwman, R. Bourne, P. Butler, I. Cadwallader-Jones, K. Campbell, T. Cooper-Benun, C. Durniak, L. Forster, P. Gilbert, M. Gonzalez, R. Heenan, A. Jackson, S. King, P. Kienzle, J. Krzywon, B. Maranville, N. Martinez, R. Murphy, T. Nielsen, L. O'Driscoll, W. Potrzebowski, S. Prescott, R. Ferraz Leal, P. Rozyczko, T. Snow, A. Washington, L. Wilkins and C. Wolf, *SasView version 5.0.6*, DOI:10.5281/zenodo.7581379.

2 L. A. Feigin and D. I. Svergun, *Structure Analysis by Small-Angle X-Ray and Neutron Scattering*, Plenum Press, New York, 1987.

3 H. Furukawa, *Physica A: Statistical Mechanics and its Applications*, 1984, **123**, 497–515.

4 H. Meier and G. R. Strobl, *Macromolecules*, 1987, **20**, 649–654.

5 T. Hashimoto, M. Takenaka and H. Jinnai, *J Appl Crystallogr*, 1991, **24**, 457–466.